Quantum phase transitions and magnetization of an integrable spin ladder with new parameters in bridging to real compounds

Zu-Jian Ying[1,2,3], Itzhak Roditi[1], Huan-Qiang Zhou[4]

1. Centro Brasileiro de Pesquisas Físicas, Rua Dr. Xavier Sigaud 150, 22290-180 Rio de Janeiro, RJ, Brasil
2. Department of Physics, Hangzhou Teachers College, Hangzhou 310012, China
3. Instituto de Física da UFRGS, Av. Bento Gonçalves, 9500, Porto Alegre, 91501-970, Brasil
4. Center for Mathematical Physics, School of Physical Sciences, The University of Queensland, 4072, Australia
()

We study the field-induced quantum phase transitions (QPT) and the relevant magnetic properties of a spin-1/2 two-leg integrable spin ladder (ISL), of which the system parameters in bridging to the real compounds are determined by setting the extra interactions in the Hamiltonian of the ISL relative to the Heisenberg spin ladder to vanish in the expectation in the ground state (GS). Such an ISL analytically has the correct leading terms of both the critical fields of the two QPT's as in the real strongly-coupled compounds: $g\mu_B H_{c1} = J_\perp - J_\parallel$ and $g\mu_B H_{c2} = J_\perp + 2J_\parallel$ in terms of the experimental leg ($J_\parallel$) and rung ($J_\perp$) interactions. The symmetric magnetization inflection point is located at $g\mu_B H_{IP} = J_\perp + J_\parallel/2$. The magnetizations for the GS and at finite temperatures, as well as the susceptibility, show good agreements in various comparisons with the finite-site exact diagonalization, the transfer-matrix renormalization group numerical result, the perturbation theory, and the compounds $(5IAP)_2CuBr_4 \cdot 2H_2O$, $Cu_2(C_5H_{12}N_2)_2Cl_4$ and $(C_5H_{12}N)_2CuBr_4$.

I. INTRODUCTION

Recently spin ladders [1] have attracted considerable interest due to increasing experimental realizations of ladder-structure compounds, such as $SrCu_2O_3$ [2], $Cu_2(C_5H_{12}N_2)_2Cl_4$ [3], $(5IAP)_2CuBr_4 \cdot 2H_2O$ [4], $(C_5H_{12}N)_2CuBr_4$ [5], etc.. Among the most interesting problems related to spin ladders are the existence of a gap, field-induced quantum phase transitions (QPT) and relevant magnetic properties. As it has been observed experimentally, strongly-coupled spin ladders are gapped and the magnetic field H induces two QPT's with two critical fields. The first critical field H_{c1} closes the gap and the second one H_{c2} fully polarizes all the spins. In terms of the weak leg ($J_\parallel$) and strong rung ($J_\perp$) interactions, the leading terms of the critical fields are $g\mu_B H_{c1} = J_\perp - J_\parallel$ and $g\mu_B H_{c2} = J_\perp + 2J_\parallel$ [6–8,3,9], which coincide with the experiments. Many spin ladder compounds can be described by the standard Heisenberg spin ladder (HSL), though some other compounds possess spin frustration and contain diagonal leg interactions. Theoretically, properties in a magnetic field have been discussed by numerical methods such as exact diagonalization [10], transfer-matrix renormalization group (TMRG) technique [11], quantum Monte Carlo simulations [12], as well as other methods for strong-coupling limit like perturbation expansions [13], bosonization [14] and mapping into XXZ Heisenberg chain [9]. Recently some effort was exerted in bridging the integrable spin ladder (ISL) [15] to real spin ladder compounds by introducing a rescaling parameter γ in the leg interaction [16,17], the high-temperature expansion (HTE) [18,19] was developed for the isotropic ISL [17] and also extended to the anisotropic ISL with an XYZ rung interaction [20]. For a real spin ladder material, it is favorable to form rung states, since it is unfavorable for the weak leg interaction to take apart the strongly-coupled rung states. It happens that the ISL is based on the permutation of the formed rung states without breaking them. Therefore, if the system parameters are properly chosen, the ISL can provide some reasonable information, while from the ISL the analysis, for its characteristic features such as the ground state (GS), excitations and the gap, the QPT's, the magnetization inflection point (IP) and thermodynamical properties in finite temperatures, is quite convenient. The rescaling parameter γ introduced in the ISL yields a gap $\Delta = J_\perp - 4J_\parallel/\gamma$ and the two critical fields $g\mu_B H_{c1} = \Delta$, $g\mu_B H_{c2} = J_\perp + 4J_\parallel/\gamma$ [16,17]. As far as the leading terms are concerned, the value $\gamma \approx 4$ for strong coupling fits the gap (and consequently H_{c1}) of the HSL [16], but the second critical field $g\mu_B H_{c2} = J_\perp + J_\parallel$ does not agree with the experiment-coinciding result $g\mu_B H_{c2} = J_\perp + 2J_\parallel$ [3,9]. Another point is that the magnetization symmetric inflection point (IP) $H_{IP} = (H_{c1} + H_{c2})/2$ takes the value $J_\perp/(g\mu_B)$ for all choices of γ, the deviation from the experimental result $H_{IP} \approx (J_\perp + J_\parallel/2)/(g\mu_B)$ will become more considerable, when the leg interaction gets stronger. A more appropriate way based on more physical origin for deciding the system parameters is lacking and expected to lay a closer bridge of the ISL to the real spin ladder compounds.

In the present paper, we shall consider an ISL where the system parameters are determined by the vanishing of the expectation value of the different interactions of the ISL relative to the HSL, for the GS in the gapped phase and the fully-polarized phase. We find that such an ISL analytically has the correct leading terms of the critical fields both at the first and the second QPT's: $g\mu_B H_{c1} = J_\perp - J_\parallel$ and $g\mu_B H_{c2} = J_\perp + 2J_\parallel$. The magnetization IP is located at $g\mu_B H_{IP} = J_\perp + J_\parallel/2$. Our result of the magnetizations for the

GS and at finite temperatures compare well both with numerical computation from the TMRG as well as the finite-spin exact diagonalization and with the experimental data for the compounds $(5IAP)_2CuBr_4\cdot2H_2O$, $Cu_2(C_5H_{12}N_2)_2Cl_4$ and $(C_5H_{12}N)_2CuBr_4$. The magnetic susceptibility coincides with the experimental data, and comparison with perturbation theory for strong coupling shows a good agreement.

II. EXACT EQUIVALENCE OF HSL AND THE ISL FOR $H \geq H_{C2}$

Many spin ladder compounds are described by the HSL with the Hamiltonian

$$\mathcal{H}_{HSL} = \mathcal{H}_{\parallel} + \mathcal{H}_{\perp} + \mathcal{M}, \tag{1}$$

$$\mathcal{H}_{\parallel} = J_{\parallel} \sum_{i=1}^{L} \mathcal{H}_{\parallel}^{i,i+1}, \ \mathcal{H}_{\parallel}^{i,i+1} = \vec{S}_i \cdot \vec{S}_{i+1} + \vec{T}_i \cdot \vec{T}_{i+1},$$

$$\mathcal{H}_{\perp} = J_{\perp} \sum_i \vec{S}_i \cdot \vec{T}_i, \ \mathcal{M} = -g\mu_B H \sum_i (S_i^z + T_i^z),$$

where $\vec{S}$ and $\vec{T}$ are spin-1/2 operators for the two legs, the three parts $\mathcal{H}_{\parallel}$, $\mathcal{H}_{\perp}$ and $\mathcal{M}$ denote the leg interaction, rung interaction and the Zeeman energy, respectively. $J_{\parallel}$ and $J_{\perp}$ are the leg and rung coupling strengths. There are totally L rungs and H is the external magnetic field.

Before considering for all values of the magnetic field, we shall first take a simple look at the fully-polarized phase and show that the HSL is equivalent to an ISL for $H \geq H_{c2}$. For convenience we label the rung singlet as $|0_i\rangle = |\uparrow\downarrow - \downarrow\uparrow\rangle_i /\sqrt{2}$ and the rung triplet as $|1_i\rangle = |\uparrow\uparrow\rangle_i$, $|2_i\rangle = |\uparrow\downarrow + \downarrow\uparrow\rangle_i /\sqrt{2}$, $|3_i\rangle = |\downarrow\downarrow\rangle_i$ where the subscript i denotes the i'th rung. The rung interaction leads to an energy $-3J_{\perp}/4$ for the singlet and $J_{\perp}/4$ for the triplet. After H_{c2} all spin are polarized so the ground state is $\Psi_{FP} = |1_1 1_2 \cdots 1_L\rangle$ for a ladder with total L rungs, which is exactly the eigenstate of the HSL $\mathcal{H}_{HSL}$.

When the field is lowered down to the critical point H_{c2} from the fully-polarized phase, spins begin to flip down. More elementally the spin flips are linear combinations of the strongly-coupled rung states. Less excitations lead to lower energy, so one the-most-favorable state will enter the GS first, which indicates the occurrence of the QPT. Since the rung state $|3\rangle$ has higher energy in the presence of the field, we only need to consider $|0\rangle$ and $|2\rangle$ for the critical point. The lowest excitation can be trapped out from a subspace where there are at most one $|0\rangle$ and $|2\rangle$, all possible neighbors collected are $\{|1_i 1_{i+1}\rangle, |1_i 0_{i+1}\rangle, |1_i 2_{i+1}\rangle, |0_i 2_{i+1}\rangle \text{ (and } |0_i 1_{i+1}\rangle, |2_i 1_{i+1}\rangle, |2_i 0_{i+1}\rangle)\}$. For all these neighbors we exactly have an equivalent relation

$$\mathcal{H}_{\parallel}^{i,i+1} = \frac{1}{2} P_{i,i+1}, \tag{2}$$

where $P_{i,i+1} \equiv (2\vec{S}_i \cdot \vec{S}_{i+1} + \frac{1}{2})(2\vec{T}_i \cdot \vec{T}_{i+1} + \frac{1}{2})$ is the permutation operator. $P_{i,i+1}$ exchanges the rung states φ_i:

$P_{i,i+1} | \varphi_i \varphi'_{i+1}\rangle = |\varphi'_i \varphi_{i+1}\rangle$. Consequently the Hamiltonian in this subspace can be rewritten as

$$\mathcal{H}_{HSL} = \sum_i \left(\frac{J_{\parallel}}{2} P_{i,i+1} + J_{\perp} \vec{S}_i \cdot \vec{T}_i - g\mu_B H(S_i^z + T_i^z) \right)$$

which is actually an ISL [15]. As there is at most one $|0\rangle$ and one $|2\rangle$, the exact eigenenergy from the Bethe ansatz approach [24] is

$$E = E_{FP} + (g\mu_B H)(N_0 + N_2)$$
$$-\frac{1}{2}J_{\parallel} \sum_{j=1}^{N_0+N_2} \frac{1}{\mu_j^2 + \frac{1}{4}} - J_{\perp} N_0, \tag{3}$$

where $E^{FP} = L\left(\frac{1}{2}J_{\parallel} + \frac{1}{4}J_{\perp} - g\mu_B H\right)$ is the fully-polarized eigenenergy, N_0 and N_2 (taking the value 0 or 1) are the numbers of states $|0\rangle$ and $|2\rangle$, respectively.

Apparently both $|0\rangle$ and $|2\rangle$ are gapful if $g\mu_B H > \max\{J_{\perp} + 2J_{\parallel}, 2J_{\parallel}\}$, and the GS is fully-polarized. The value $\mu = 0$ corresponds to the critical field $g\mu_B H_{c2} = \max\{J_{\perp} + 2J_{\parallel}, 2J_{\parallel}\}$, which reaches the same result deduced from the instability of spin wave spectrum in the ferromagnetic phase [3] and that obtained from mapping onto an XXZ Heisenberg chain [9]. The expression of the saturation point is exact [3], more exactly speaking, for an even number of rungs. The one-particle Bethe ansatz wavefunction corresponding to $\mu = 0$ provides

$$\Psi_{c2} = \sum_{i=1}^{L} (-1)^i |1_1 1_2 \cdots b_i \cdots 1_L\rangle, \tag{4}$$

where $b_i = 0, 2$ according to favorable energy. For antiferromagnetic spin ladder with positive $J_{\perp}$ and $J_{\parallel}$, $|2\rangle$ has higher excitation energy, then b_i is the singlet $|0\rangle$ and $g\mu_B H_{c2} = J_{\perp} + 2J_{\parallel}$. The Ψ_{c2} will be used in our further discussion. For an odd number of periodic rungs, the term $2J_{\parallel}$ in the critical expression is replaced by $(1 - \cos[(1 - 1/L)\pi]) J_{\parallel}$, as $\mu = 0$ is not the solution in periodic boundary conditions. But this size effect will completely disappear in thermodynamical limit.

III. ISL IN BRIDGING TO THE COMPOUNDS IN ALL FIELD VALUES

After the simple look at the fully-polarized phase in the previous section, we proceed to discuss all values of the field applied on an antiferromagnetic spin ladder. The relation $\mathcal{H}_{\parallel}^{i,i+1} = \frac{1}{2} P_{i,i+1}$ from (2) does not hold for neighbors $|0_i 0_{i+1}\rangle$, $|2_i 2_{i+1}\rangle$ or $|1_i 3_{i+1}\rangle$, though it is exact for all the other kinds of neighbor states. To find a model effective for all value of fields, we shall consider such an ISL with the difference in $\mathcal{H}_0$

$$\mathcal{H}_{ISL} = \mathcal{H}_0 + \mathcal{H}_{\perp} + \mathcal{M}, \tag{5}$$
$$\mathcal{H}_0 = J_{\parallel} \sum_i \mathcal{H}_0^{i,i+1}, \ \mathcal{H}_0^{i,i+1} = \mathcal{H}_{\parallel}^{i,i+1} + \mathcal{H}_{extra}^{i,i+1},$$

where

$$\mathcal{H}_{extra}^{i,i+1} = \frac{P_{i,i+1}}{\gamma} - \mathcal{H}_{\parallel}^{i,i+1} + \frac{\alpha}{2}(\vec{S}_i \cdot \vec{T}_i + \vec{S}_{i+1} \cdot \vec{T}_{i+1}) + c. \tag{6}$$

The rung interaction part $\mathcal{H}_{\perp}$ and Zeeman term $\mathcal{M}$ are exactly the same as the HSL $\mathcal{H}_{HSL}$. If $\mathcal{H}_{extra}^{i,i+1} = 0$, the $\mathcal{H}_0^{i,i+1}$ will reduce to the leg interaction of the HSL. The extra part $\mathcal{H}_{extra}^{i,i+1}$ makes the model integrable, but the biquadratic exchange $\vec{S}_i \cdot \vec{S}_{i+1}\vec{T}_i \cdot \vec{T}_{i+1}$ [21] in $P_{i,i+1}$ does not appear in the HSL, though it is as weak as the leg interaction. We set and balance the parameters γ, α and c to reduce its influence. To minimize its extra effect, we consider in such a way that it vanishes in expectation

$$\langle J_{\parallel} \sum_{i=1}^{L} \mathcal{H}_{extra}^{i,i+1} \rangle = 0, \tag{7}$$

as much as possible in the GS. Our consideration aims to make the model exactly soluble on one hand, while on the other hand, the extra effect is minimized as much as possible.

More complicated balance terms such as $S_i^z T_i^z$, $S_i^z + T_i^z$ can be taken into account in $\mathcal{H}_{extra}^{i,i+1}$ but they break the isotropy. Here we consider the simplest case (6) which preserves the isotropy when it is giving quite good results. To see the integrability, the Hamiltonian can be rewritten as

$$\mathcal{H}_{ISL} = J_{\parallel} \sum_i (\frac{P_{i,i+1}}{\gamma} + c) + (J_{\perp} + \alpha J_{\parallel}) \sum_i \vec{S}_i \cdot \vec{T}_i + \mathcal{M} \tag{8}$$

where $P_{i,i+1}$ forms the permutation operator in the SU(4) integrable model [22,23] and $\mathcal{M}$ is the Zeeman term as in the HSL. The model (8) essentially is an ISL [15] which can be exactly solved by Bethe ansatz approach [24]. The exact eigenenergy reads

$$E = -\frac{J_{\parallel}}{\gamma} \sum_j^{M^{(1)}} \frac{1}{\mu_j^{(1)2} + \frac{1}{4}} + \sum_{k=0}^{3} E_k N_k + (\frac{1}{2} + c) L J_{\parallel}, \tag{9}$$

$$E_0 = -\frac{3}{4}(J_{\perp} + \alpha J_{\parallel}), \ E_1 = \frac{1}{4}(J_{\perp} + \alpha J_{\parallel}) - g\mu_B H,$$

$$E_2 = \frac{1}{4}(J_{\perp} + \alpha J_{\parallel}), \ E_3 = \frac{1}{4}(J_{\perp} + \alpha J_{\parallel}) + g\mu_B H,$$

where E_k is the single-rung energy of the singlet (E_0) and triplet (E_1, E_2, E_3), N_k is the total rung number in the corresponding rung states. The rung state with lowest E_k is chosen as the reference state, $M^{(1)}$ is the total number of rungs occupied by the other rung states. The singlet is chosen as the reference state before the IP $g\mu_B H_{IP} = (J_{\perp} + \alpha J_{\parallel})$ (decided by $E_0 = E_1$), while $|1\rangle$ is the reference state thereafter. The gapped phase lies in the former case and the fully-polarized phase locates in the latter.

The gapped phase of the ISL is composed of the singlet. The magnetic field lowers the energy of the triplet component $|1\rangle$ which enters the GS when the gap is closed at the first QPT. Further increase of the field brings all the components of the singlet out of the GS and another gap opens at the second QPT (we refer the gapped phase to be at $H < H_{c1}$, though the fully-polarized phase is also gapped). Since both the gapped phase and the fully-polarized phase only consist of one rung state ($|0\rangle$ or $|1\rangle$, respectively), which is chosen as the reference state, $M^{(1)}$ in these two phases corresponds to the number of the excitations to the other three components. Then from the eigenenergy (9), it is very easy to find the excitation gap and the two critical fields

$$g\mu_B H_{c1} = (J_{\perp} + \alpha J_{\parallel}) - \frac{4}{\gamma} J_{\parallel},$$

$$g\mu_B H_{c2} = (J_{\perp} + \alpha J_{\parallel}) + \frac{4}{\gamma} J_{\parallel}, \tag{10}$$

which, respectively, closes the gap of the gapped phase and open the gap of the fully-polarized phase. The $4/\gamma$ terms come from the lowest energy in the excitation band, $\mu_j^{(1)} = 0$ corresponds to the bottom of the energy band. The critical fields as well as the IP realize the relation $H_{IP} = \frac{1}{2}(H_{c1} + H_{c2})$, which is the magnetization symmetric point and agrees with the experiments, as discussed in the following.

Experimentally strongly-coupled spin ladder compounds have two similar QPT's, separating the application of the external magnetic field into three phases. As usually described by the HSL, the fully-polarized state Ψ_{FP} exactly is the system GS after the second phase transition, while the singlet is the most favorable state and dominates overwhelmingly in the gapped phase before the occurrence of the first QPT for the antiferromagnetically strongly-coupled real spin ladder compounds.

Among the total three phases, the extra-interaction effect of the ISL can be minimized explicitly in two phases, gapped phase and the fully-polarized phase. Fulfilling the relation (7) in these two phase gives rise to

$$\frac{1}{\gamma} - \frac{1}{2} + \frac{1}{4}\alpha + c = 0, \ H > H_{c2}; \tag{11}$$

$$\frac{1}{\gamma} - \frac{3}{4}\alpha + c = 0, \ H < H_{c1}, \tag{12}$$

where the term $1/2$ in the former equation comes from the expectation of the HSL leg interaction, while in the latter equation this expectation vanishes in the singlet phase. The solution is direct to obtain and we yield to the limitations

$$\frac{1}{\gamma} = \frac{3}{8} - c, \ \alpha = \frac{1}{2}. \tag{13}$$

Under these parameters, the GS has the exact equivalence $\mathcal{H}_{HSL} = \mathcal{H}_{ISL}$ for the fully-polarized phase $H >$

H_{c2} and the expectation equivalence $\langle \mathcal{H}_{HSL} \rangle = \langle \mathcal{H}_{ISL} \rangle$ for the gapped singlet phase $H < H_{c1}$. Then the IP is determined from the definite α in (13)

$$g\mu_B H_{IP} = J_\perp + \frac{1}{2} J_\parallel, \qquad (14)$$

which, as it turns out in the following comparisons, produces well the experimental value and TMRG numerical result. Note here that this experiment-coinciding IP expression is an analytic result from our consideration, and instead of from empirical parameter choosing, the presence of the term $\frac{1}{2} J_\parallel$ comes from the only requirement on the extra-interaction-effect minimizing (7) of the above two phases. We shall decide more definitely the parameter γ by considering the critical points of the QPT's.

A. Equivalence at the 2nd QPT

Since the exact analysis for the HSL is available at the second QPT as discussed in the previous section, we first consider such a case that the extra interactions of the ISL also vanish at the second critical point, in addition to the requirement on the gapped phase and fully-polarized phase. Although $\mathcal{H}_{extra}^{i,i+1}$ does not vanish for a single neighbor-site pairs $|1_i 0_{i+1}\rangle$ at H_{c2}, the action of these extra terms together can cancel each other. In fact, noticing the relation (2) for the rung-state neighbors $|1_i 1_{i+1}\rangle$ and $|1_i 0_{i+1}\rangle$ involved at the second critical point, one can easily obtain

$$\sum_{i=1}^{L} \mathcal{H}_{extra}^{i,i+1} \Psi_{c2} = [(\frac{1}{\gamma} - \frac{1}{2} + \frac{\alpha}{4})(L-4) + cL] \Psi_{c2}. \quad (15)$$

Setting the extra-interaction effect to vanish $\sum_{i=1}^{L} \mathcal{H}_{extra}^{i,i+1} \Psi_{c2} = 0$, in addition to the limitations (13) from the afore-discussed two phases, leads us to the definite parameters

$$\gamma = \frac{8}{3}, \; \alpha = \frac{1}{2}, \; c = 0. \qquad (16)$$

Thus the relation (2) is replaced by $\mathcal{H}_\parallel^{i,i+1} = \mathcal{H}_0^{i,i+1}$ for fully-polarized phase $H > H_{c2}$ and $\sum_i \mathcal{H}_\parallel^{i,i+1} = \sum_i \mathcal{H}_0^{i,i+1}$ at the critical point H_{c2}. Such a simple consideration immediately gives the two critical fields

$$g\mu_B H_{c1} = J_\perp - J_\parallel,$$
$$g\mu_B H_{c2} = J_\perp + 2J_\parallel. \qquad (17)$$

As it is expected, H_{c2} is the same exact result as we discuss in the previous section. Note that here H_{c1} for the first QPT is actually composed of the leading terms from the perturbation theory and has been often used in experiments, while we have not imposed any limitation on the first QPT and it is a by-product of the consideration of the second QPT.

The magnetization can be obtained by thermodynamical Bethe ansatz (TBA) [25,26] which is also very convenient for analysis of the field-induced QPT's [16,27,20]. For the ISL under consideration, the magnetization between the two critical fields in zero-temperature is decided by the following TBA equations of the dressed energy and density,

$$\epsilon^{(1)} = g^{(1)} - 2\pi a_1 - a_2 * \epsilon^{(1)-},$$
$$\rho^{(1)} = a_1 - a_2 * \rho^{(1)-}, \qquad (18)$$

where $g^{(1)} = \pm\gamma[(1+\alpha)J_\perp - g\mu_B H]/J_\parallel$ for $\pm(H_{IP}-H) > 0$, $a_n(\mu) = [n/(\mu^2 + n^2/4)]/(2\pi)$, and the symbol $*$ denotes the convolution. The Fermi sea with negative dressed energy $\epsilon^{(1)-}$ forms the system GS. Here the GS only involves one branch of dressed energy, since the GS of the ISL is composed of the singlet in the absence of the field, while only the component $|1\rangle$ is lowered in energy level and brought down to the GS by the applied field. Correspondingly the gap of the excitation to the component $|2\rangle$ and $|3\rangle$ never closes during the gapless competition between $|0\rangle$ and $|1\rangle$ in the GS. We present an example of the GS magnetization in Fig.1. The symbols are data figured out from Ref. [10] in the study by Lanczos exact diagonalization on 2×12 and 2×16 HSL with periodic boundary conditions, the ratio of the leg and rung interaction strength is $J_\parallel/J_\perp = 0.2$. The solid curve is our result which coincides with the finite-site exact diagonalization. There is some small discrepancy at the first QPT due to existence of higher-order terms in H_{c1} (the discrepancy will be reduced when the higher-order terms are picked up, as one will see from GS magnetization compared with T=0.02 TMRG result in Fig.5 and Fig.7). As our consideration provides the same H_{c1} and H_{c2} as the HSL in leading terms, the coincidence of our result with the experiments is also expected. Two examples are given in Fig.2A and B, respectively for the compound $Cu_2(C_5H_{12}N_2)_2Cl_4$ [3] with ratio $J_\parallel/J_\perp \approx 0.18$ and $(C_5H_{12}N)_2CuBr_4$ [5] with $J_\parallel/J_\perp \approx 0.29$.

The high-temperature expansion (HTE) [18,19] has been developed for the isotropic ISL [17]. Then the temperature-dependent free energy per spin takes the form

$$f = -\frac{1}{2} T \sum_{n=0}^{\infty} C_n (\frac{J_\parallel}{\gamma k_B T})^n, \qquad (19)$$

where the expansion is carried out for per rung and the factor $1/2$ is added for per spin, k_B is the Boltzmann constant. We present some orders of coefficients,

$$C_0 = \ln Q_+, \; C_1 = \frac{2Q}{Q_+^2}, \; C_2 = \frac{3Q}{Q_+^2} - \frac{6Q^2}{Q_+^4} + \frac{3Q_-}{Q_+^3},$$

$$C_3 = \frac{10Q}{3Q_+^2} - \frac{18Q^2}{Q_+^4} + \frac{80Q^3}{3Q_+^6} + \frac{8Q_-}{Q_+^3} - \frac{24QQ_-}{Q_+^5} + \frac{4}{Q_+^4},$$

$$C_4 = \frac{35Q}{12Q_+^2} - \frac{205Q^2}{6Q_+^4} + \frac{120Q^3}{Q_+^6} - \frac{140Q^4}{Q_+^8} + \frac{55Q_-}{4Q_+^3}$$

$$-\frac{100QQ_-}{Q_+^5} + \frac{180Q^2Q_-}{Q_+^7} - \frac{45Q_-^2}{2Q_+^6} + \frac{15}{Q_+^4} - \frac{40Q}{Q_+^6},$$

where

$$Q = 2\cosh(\frac{1}{2}\beta\widetilde{J}) + 4\cosh(\frac{1}{2}\beta\widetilde{J})\cosh(\beta h),$$

$$Q_\pm = 2e^{(\pm\beta\widetilde{J}/4)}\cosh(\frac{1}{2}\beta\widetilde{J}) + 2e^{(\mp\beta\widetilde{J}/4)}\cosh(\beta h),$$

$h = g\mu_B H$, $\widetilde{J} = (J_\perp + \alpha J_\parallel)$ and $\beta = 1/(k_B T)$. One can get higher orders for lower temperatures. We compare our result of (16) with the compound $(5IAP)_2CuBr_4\cdot2H_2O$ [4], with ratio $J_\parallel/J_\perp \approx 0.077 \pm 0.015$, the magnetizations $M = -\partial F/\partial H$ and the magnetic susceptibility $\chi = -\partial^2 F/\partial H^2$ are presented in Fig.3 and Fig.4, respectively. The comparison shows a good agreement with the experiments. The unit of the susceptibility in comparing the experiment is determined by the Curie constant C, which can be clearly seen when we expand the susceptibility in (27). The Curie constant is decided, usually for molar susceptibility, when the g factor is measured by the experiment. For the compound $Cu_2(C_5H_{12}N_2)_2Cl_4$ [3], we have shown in Fig.2B the coincidence of our GS magnetization with the experimental magnetization of the lowest available temperature. This compound possesses nonlinear torque magnetization [29] and possible weak diagonal interaction [10], which may be the possible reason that causes the observed asymmetric magnetizations at different higher temperatures. So here we shall not compare the magnetizations for this compound at higher temperatures. The compound $(C_5H_{12}N)_2CuBr_4$ [5] has stronger leg interaction ($J_\parallel/J_\perp \sim 0.3$), the higher-order terms of the gap become more considerable. The small difference resulted from the high order terms can be seen from Fig.2B, the dotted line and the solid one are the magnetizations in the absence and presence of the high-order terms, respectively. In the following we shall pick up the high-order terms.

B. Fitting of the 1st QPT

Up to now our consideration has exhibited the correct leading terms of the critical fields. When the leg interaction is stronger, the higher-order terms in the gap (equal to $g\mu_B H_{c1}$) become more considerable. On the other hand, the fluctuation $\langle\mathcal{H}_{HSL}^2\rangle - \langle\mathcal{H}_{HSL}\rangle^2$ in the singlet phase is very large, treatment of the first QPT may influence the system properties more sensitively than the second QPT. Unlike in the second QPT, the exact solution of the HSL is not available in the first QPT, requiring $\sum_i \mathcal{H}_{extra}^{i,i+1}\Psi_{c1} = 0$ is not explicitly executable. So we directly adjust the parameters to fit the gap, which is also a result of $\langle\mathcal{H}_{HSL}\rangle = \langle\mathcal{H}_{ISL}\rangle$. The higher orders terms in the gap of the HSL converge slowly in the perturbation theory, but it was found [12] that a two-parameter gap Δ_0 fits the numerical data of Greven *et al.* [30] very well

$$\Delta_0 = J_\perp - J_\parallel + dJ_\parallel, \ d = a(\frac{J_\parallel}{J_\perp}) + b(\frac{J_\parallel}{J_\perp})^2, \quad (20)$$

where $a = 0.6878$, $b = -0.1861$. The $dJ_\parallel$ comes from the high-order terms in the gap and here we have used a label d for our convenience. Setting

$$\frac{1}{\gamma} = \frac{3}{8} - \frac{d}{4}, \ \alpha = \frac{1}{2}, \ c = \frac{d}{4}, \quad (21)$$

will give rise to this gap at the same time when the requirement in (13) of the ISL is fulfilled. In Fig.5 we compare the magnetizations with the TMRG numerical result [11] in various temperatures, for $J_\parallel = 1$, $J_\perp = 5.28$. The solid lines are plotted according to the corresponding temperatures of the TMRG data, the broken line is plotted at T= 0 compared with the lowest temperature T=0.02 TMRG result. As one can see, the agreement is quite good for all the temperatures. For the comparison with the experiment, Fig.6 presents the magnetizations for the spin ladder compound $(C_5H_{12}N)_2CuBr_4$ [5] with a stronger leg interaction ($J_\parallel/J_\perp \approx 0.29$, $d \approx 0.18$). As the HTE is not valid for 0.7K, we also calculate the magnetization of GS (0.0K) by TBA, a more clear comparison has been presented in 2B. The figure demonstrates a good agreement of our result with the experiment. The susceptibility in a low field is given in the inset, our result in the solid line coincides with the experimental observation except for some small deviation at the hump.

The interesting IP is an invariant point of the magnetizations at low temperatures. The compound $(5IAP)_2CuBr_4\cdot2H_2O$ [4] in Fig.3 indicates the IP, though it suffers from the impurities. As the compound $(C_5H_{12}N)_2CuBr_4$ is free of the impurity or diagonal interaction, it exhibits an unambiguous IP at the half-saturation. The TMRG numerical calculation for the theoretically ideal HSL also shows the IP. From the ISL, it is direct to understand the IP [20,16,17]. Two reasons are both necessary for the IP: (i) equal energy of the only two components competing in the GS; (ii) large excitation gap relative to the temperatures. Actually only two components, the singlet $|0\rangle$ and the triplet component $|1\rangle$, compete in the GS, as we mentioned below the dressed energy equation. The IP locates at the point where the reference state in an increasing field converts from $|0\rangle$ to $|1\rangle$. At this point the two components have the same rung energy $E_0 = E_1$ and same proportion $N_0 = N_1$ in the GS. The excitations to the other components $|2\rangle$ to $|3\rangle$ are gapful, the gap are exactly available [20]

$$\Delta_{IP} = (J_\perp + \alpha J_\parallel) - (2\ln 2)J_\parallel/\gamma, \quad (22)$$

which is large due to the strong rung coupling $J_\perp$. Low temperatures can hardly stimulate excitations to $|2\rangle$ or $|3\rangle$, while each of $|0\rangle$ and $|1\rangle$ with the same energy still occupies half the total rungs. As a result, the IP is invariant with a half-saturation magnetization under low temperatures. Higher temperatures will excite $|2\rangle$ as well as

$|3\rangle$ and lower the magnetization, consequently the magnetization curves do not go through the IP, as one can see partly from the temperature T=2.5 and more clearly from T= 5.0, 10 in Fig.5. The location of the IP is well produced by our analytic expression (14) for the compound and the TMRG data. For the unambiguous IP of the compound $(C_5H_{12}N)_2CuBr_4$ ($g = 2.13$, $J_\perp = 13.3$K, $J_\parallel = 3.8$K) our result $H_{IP} = 10.6$T is identical with the experimental observation; the result for $J_\perp = 5.28$, $J_\parallel = 1$ from TMRG keeping 200 optimal states provides an IP at $H_{IP} \approx 5.83$ ($H_{c1} \approx 4.38, H_{c2} \approx 7.28$ and $g\mu_B$ is incorporated in the field as in Ref. [11]) when our result is $H_{IP} = 5.78$ with a very minor discrepancy about 0.9%.

C. Fitting both the two critical fields

Under the parameters (21) for fitting the gap, the extra interactions at the second critical field will be $J_\parallel \sum_{i=1}^{L} \mathcal{H}_{extra}^{i,i+1} \Psi_{c2} = -dJ_\parallel \Psi_{c2}$, which does not vanish though it is small. Nevertheless, this can be also resolved by more consideration. Previously we only take the dominant singlet component into account in the gapped phase of the HSL, as a simple physical picture as in the ISL. When the HSL-type leg interaction becomes less weak, small amount of other components will be mixed into the gapped singlet phase of the strong coupling limit. Therefore the average per-leg expectation value of the HSL leg interaction does not vanish as in a pure singlet phase. This contributes to another modification parameter δ. As we are using the ISL to describe the compounds, the (12) becomes

$$\frac{1}{\gamma} - \frac{3}{4}\alpha + c = \delta, \ H < H_{c1}, \qquad (23)$$

instead. In limitation (12), δ is null in our previous simpler consideration that singlet component dominates overwhelmingly in the strongly-coupled HSL. Combining (23) in the gapped phase, the gap fitting $g\mu_B H_{c1} = \Delta_0$ and the extra-interaction minimizing (11) in the fully-polarized phase, one gets

$$\frac{1}{\gamma} = \frac{3}{8} - \frac{d+\delta}{4}, \ \alpha = \frac{1}{2} - \delta, \ c = \frac{\delta}{2} + \frac{d}{4}. \qquad (24)$$

If setting $\delta = -d/2$, one will regain the vanishing of the extra-interaction $\sum_{i=1}^{L} \mathcal{H}_{extra}^{i,i+1} \Psi_{c2} = 0$ for the second critical field. In such case we will have the critical fields

$$g\mu_B H_{c1} = J_\perp - J_\parallel + dJ_\parallel, \ g\mu_B H_{c2} = J_\perp + 2J_\parallel, \quad (25)$$

as well as a new IP

$$g\mu_B H_{IP} = J_\perp + \frac{1}{2}J_\parallel + \frac{d}{2}J_\parallel. \qquad (26)$$

For the compound $(C_5H_{12}N)_2CuBr_4$ [5], these results does not give improvement to the magnetizations except

some small improvement at the peak of the low-field susceptibility (given in the inset of the Fig.6). But for the theoretically ideal HSL under the couplings $J_\perp = 5.28$, $J_\parallel = 1$, the value $d \approx 0.124$ from (20) gives the IP $g\mu_B H_{IP} = 5.84$, which minimizes the discrepancy from the TMRG result $g\mu_B H_{IP} = 5.83$ [11]. As our previous considerations with simple parameters have given quite good results, here we just give a comparison for the GS magnetization with the TMRG data in Fig.7.

D. Susceptibility compared with perturbation theory of HSL

In bridging to the experimental data, the unit is a problem needing some special attention. The unit of the susceptibility can be clarified if the expansion is carried out. One can obtain the expansions of the susceptibility for N spins easily from the free energy expression, the lowest two orders take the form

$$\chi = \frac{C}{T}\left[1 - \frac{1}{4k_BT}\left(J_\perp + (\frac{2}{\gamma} + \alpha)J_\parallel\right) + \mathcal{O}(\frac{1}{T^2})\right] \quad (27)$$

where $C = Ng^2\mu_B^2/(4k_B)$ is the Curie constant. In the expression (27) the part in the square brackets is dimensionless. The Curie constant is provided by the experiments corresponding to a measured value of g, e.g., $C = 0.412$ emu K/mol for the compound $(5IAP)_2CuBr_4 \cdot 2H_2O$ ($g = 2.1$) [4]. As one knows, the lowest order $\chi = C/T$ is the Curie law, which guarantees the coincidence with the experimental data in high temperatures ($T \to 100$K for the compounds discussed in the present paper). Comparing (27) with the Curie-Weiss Law $\chi = C/(T-\Theta)$ implies a Curie-Weiss temperature $\Theta_{ISL} = -[J_\perp + (2/\gamma + \alpha)J_\parallel]/4$ for the ISL (8). The HSL has a Curie-Weiss temperature $\Theta_{HSL} = -(J_\perp + 2J_\parallel)/4$ [12]. Our parameters $\gamma = 8/3$, $\alpha = 1/2$ provide $\Theta_{ISL} = -(J_\perp + 5J_\parallel/4)/4$, which is close to that of the HSL. The difference of Θ_{ISL} from Θ_{HSL} will be more ignorable when the leg interaction $J_\parallel$ is relatively small in a strongly-coupled spin ladder, which coincides with the good agreement of susceptibility for the compound $(5IAP)_2CuBr_4 \cdot 2H_2O$.

For the strongly-coupled HSL, it was found that the expression of zero-field susceptibility derived from perturbation theory [12,13],

$$\chi = \frac{4C}{T}\left\{\frac{1}{3+e^{\mathcal{B}}} - \frac{J_\parallel}{J_\perp}\left[\frac{2\mathcal{B}}{(3+e^{\mathcal{B}})^2}\right]\right.$$
$$-\left(\frac{J_\parallel}{J_\perp}\right)^2\left[\frac{3\mathcal{B}(e^{2\mathcal{B}}-1) - \mathcal{B}^2(5+e^{2\mathcal{B}})}{4(3+e^{\mathcal{B}})^3}\right]$$
$$-\left(\frac{J_\parallel}{J_\perp}\right)^3\left[\frac{3\mathcal{B}(e^{2\mathcal{B}}-1)}{8(3+e^{\mathcal{B}})^3}\right.$$
$$\left.\left.-\frac{9\mathcal{B}^2e^{\mathcal{B}}(1+3e^{\mathcal{B}}) - \mathcal{B}^3(7e^{2\mathcal{B}} - 9e^{\mathcal{B}} - 12)}{12(3+e^{\mathcal{B}})^4}\right]\right\}, \quad (28)$$

6

reproduces with high accuracy the quantum Monte Carlo simulations [12], as long as the ratio $J_\parallel/J_\perp$ does not exceed 0.1. The definition $\mathcal{B} = J_\perp/(k_B T)$ is utilized in (28). We compare our result of the susceptibility with (28) of the HSL in Fig.8. For more clarity of unit, we use the susceptibility scaled by the Curie constant. The comparison for $J_\parallel/J_\perp = 0.1$ shows that our result is in a very good agreement with that of HSL, the coincidence will be even better for $J_\parallel/J_\perp < 0.1$.

IV. SUMMARY

We have studied the quantum phase transitions, the magnetizations and susceptibility of an integrable spin ladder (ISL) by proposing a new way in deciding the system parameters to build closer connection of the ISL with the real compounds. The system parameters are chosen to make the extra interactions of the ISL relative to the Heisenberg spin ladder (HSL) vanish in the expectation of the ground state, especially for the gapped phase and fully-polarized phase. The analytic critical fields of such an ISL have the same leading terms as those of the experimental observations and the HSL: $g\mu_B H_{c1} \approx J_\perp - J_\parallel$ and $g\mu_B H_{c2} \approx J_\perp + 2J_\parallel$, accompanied by the symmetric magnetization inflection point with the location analytically at $g\mu_B H_{IP} = J_\perp + J_\parallel/2$ (another result $g\mu_B H_{IP} = J_\perp + J_\parallel/2 + dJ_\parallel/2$). A variety of comparisons have been made with other numerical results and the experiments. The magnetizations coincide with the finite-site exact diagonalization of the HSL for the GS, and with the TMRG numerical result for full temperatures. For experiments, the magnetizations agree well with the compounds $(5IAP)_2CuBr_4 \cdot 2H_2O$, $Cu_2(C_5H_{12}N_2)_2Cl_4$ and $(C_5H_{12}N)_2CuBr_4$, with the leg and rung coupling ratio $J_\parallel/J_\perp$ around 0.1, 0.2 and 0.3, respectively. The susceptibility with the clarified unit also coincides with the strongly-coupled compound as well as perturbation theory. The coincidence in the magnetization and susceptibility also makes it possible to discuss the specific heat for the whole process of the field application, we shall present the discussion in another paper. Our method may also be helpful for other integrable models in bridging to the experiments and real compounds.

V. ACKNOWLEDGMENTS

[1] E. Dagotto and T. M. Rice, Science **271**, 618 (1996); E. Dagotto, Rep. Prog. Phys. **62**, 1525 (1999).
[2] M. Azuma, Z. Hiroi, M. Takano, K. Ishida and Y. Kitaoka, Phys. Rev. Lett. **73**, 3463 (1994).
[3] G. Chaboussant, P. A. Crowell, L. P. Lévy, O. Piovesana, A. Madouri, and D. Mailly, Phys. Rev. B **55**, 3046 (1997).
[4] C. P. Landee, M. M. Turnbull, C. Galeriu, J. Giantsidis, and F. M. Woodward, Phys. Rev. B **63**, 100402 (2001).
[5] B. C. Watson, V. N. Kotov, M. W. Meisel, D. W. Hall, G. E. Granroth, W. T. Montfrooij, S. E. Nagler, D. A Jensen, R. Backov, M. A. Petruska, G. E. Fanucci, and D. R. Talham, Phys. Rev. Lett. **86**, 5168 (2001).
[6] T. Barnes, E. Dagotto, J. Riera, and E. S. Swanson, Phys. Rev. B **47**, 3196 (1993).
[7] M. Reigrotzki, H. Tsunetsugu, and T.M. Rice, J. Phys.: Condens. Matter **6**, 9235 (1994).
[8] Zheng Weihong, V. Kotov, and J. Oitmaa, Phys. Rev. B **57**, 11439 (1998).
[9] F. Mila, Eur. Phys. J. B **6**, 201 (1998).
[10] C. A. Hayward, D. Poilblanc, and L. P. Lévy, Phys. Rev. B **54**, 12649 (1996).
[11] X.-Q. Wang and L. Yu, Phys. Rev. Lett. **84**, 5399 (2000).
[12] D.C. Johnston, M. Troyer, S. Miyahara, D. Lidsky, K. Ueda, M. Azuma, Z. Hiroi, M. Takano, M. Isobe, Y. Ueda, M.A. Korotin, V.I. Anisimov, A.V. Mahajan, and L.L. Miller, cond-mat/0001147.
[13] Q. Gu, D.-K. Yu, and J.-L. Shen, Phys. Rev. B **60**, 3009 (1999).
[14] R. Chitra and T. Giamarchi, Phys. Rev. B **55**, 5816 (1997).
[15] Y. Wang, Phys. Rev. B **60**, 9236 (1999).
[16] M.T. Batchelor, X.W. Guan, A. Foerster and H.Q. Zhou, New J. Phys. **5**, 107 (2003).
[17] M. T. Batchelor, X.-W. Guan, N. Oelkers, K. Sakai, Z. Tsuboi, and A. Foerster, Phys. Rev. Lett. **91**, 217202 (2003).
[18] M. Shiroishi and M. Takahashi, Phys. Rev. Lett. **89**, 117201 (2002).
[19] Z. Tsuboi, J. Phys. A **36**, 1493 (2003).
[20] Z.J. Ying, I. Roditi, A. Foerster and B. Chen, cond-mat/0403520.
[21] In weak-coupling ladders the four-spin interactions can be generated by phonons or Coulomb repulsion between holes, see, e.g., A. A. Nersesyan and A. M. Tsvelik, Phys. Rev. Lett. **78**, 3939 (1997).
[22] Y.Q. Li, M. Ma, D.N. Shi and F.C. Zhang, Phys. Rev. Lett. **81**, 3527 (1998).
[23] Y.Q. Li, M. Ma, D.N. Shi and F.C. Zhang, Phys. Rev. B **60**, 12781 (1999).
[24] B. Sutherland, Phys. Rev. B **12**, 3795 (1975).
[25] C.N. Yang and C.P. Yang, J. Math. Phys. **10**, 1115(1969); M. Takahashi, Prog. Theor. Phys. **46**, 401 (1971); P. Schlottmann, Phys. Rev. B **33**, 4880 (1986).
[26] H. Frahm and V. E. Korepin, Phys. Rev. B **42**, 10553 (1990).
[27] Z.J. Ying, A. Foerster, X.W. Guan, B. Chen, and I. Roditi, cond-mat/0308443, revised, to appear in Eur. Phys. J. B.

[28] As the value of the gap Δ is not provided in Ref. [10] due to its variation for the presented various couplings, we take the exact second critical point $g\mu_B H_{c2} = J_\perp + 2J_\parallel$ as a reference instead, marked by the symbol "*".

[29] P. Crowell, A. Madouri, M. Specht, G. Chaboussant, D. Mailly, and L.P. Lévy, Rev. Sci. Inst. **67**, 4161 (1996).

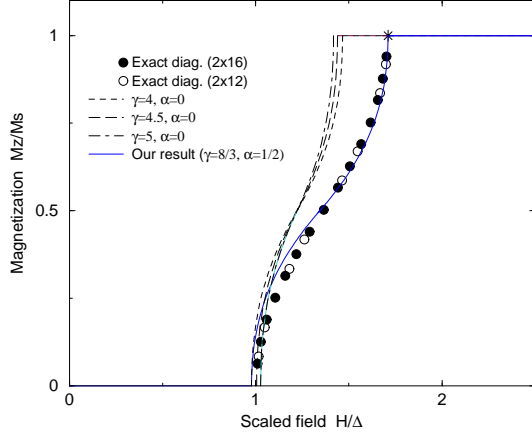[30] M. Greven, R.J. Birgeneau, and U.-J. Wiese, Phys. Rev. Lett. **77**, 1865 (1996).

FIG. 1. Magnetization versus the scaled magnetic field for the ground state (GS) (T=0.0K), $J_\parallel/J_\perp = 0.2$. The symbols are result of Lanczos exact diagonalization on 2×12 and 2×16 Heisenberg spin ladder (HSL) with periodic boundary conditions, the data are figured out from Ref.[10]. Δ is the gap of the HSL [28]. Our result (solid curve) from $\gamma = 8/3$ and $\alpha = 1/2$ coincides with that of the exact diagonalization, there is some small discrepancy at the first QPT due to existence of higher orders terms in H_{c1}. The dashed lines present result of some choices from an adjustable γ and $\alpha = 0$, they all go through a same half-saturation point away from the exact diagonalization data.
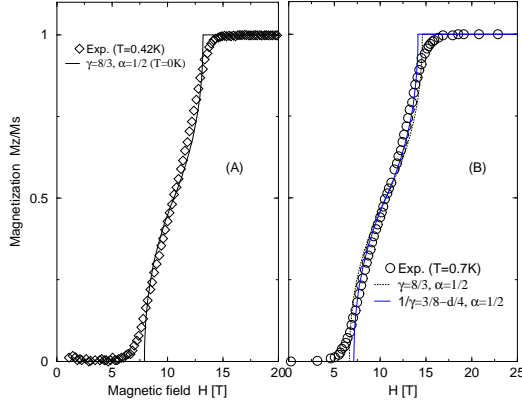

FIG. 2. (A). Groundstate magnetization versus the magnetic field in comparison with the compound $Cu_2(C_5H_{12}N_2)_2Cl_4$ [3], $g_z = 2.03$, $J_\perp = 13.2$K, $J_\parallel = 2.4$K, $J_\parallel/J_\perp = 0.18$. The symbols are experimental magnetization for the lowest available temperature (0.42K). The solid line is the groundstate (T=0.0K) magnetization calculated from our consideration with $\gamma = 8/3$ and $\alpha = 1/2$. (B). Groundstate magnetization compared with another compound $(C_5H_{12}N)_2CuBr_4$ [5], $g = 2.13$, $J_\perp = 13.3$K, $J_\parallel = 3.8$K, $J_\parallel/J_\perp = 0.29$. The temperature of the experimental data is 0.7K. The dotted line is the result of $\gamma = 8/3$ and $\alpha = 1/2$, while the solid line is the result including the high order terms in the gap, $1/\gamma = 3/8 - d/4$ and $\alpha = 1/2$. The parameter d is given by (20) under certain values of $J_\perp$ and $J_\parallel$.
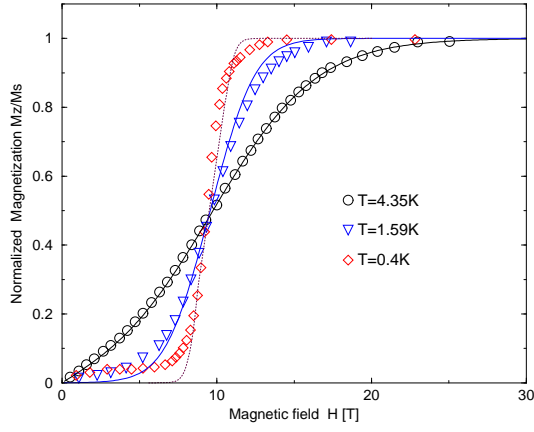
FIG. 3. Magnetizations versus the magnetic field at different temperatures for the compounds $(5IAP)_2CuBr_4\cdot2H_2O$, $g = 2.1$, $J_\perp = 13.0K$, $J_\parallel = 1.0K$. The data in symbols are the experimental result[4], the lines are plotted from our theoretical calculation ($\gamma = 8/3$ and $\alpha = 1/2$). The compound contains a considerable amount of impurities, which can be seen obviously in the magnetization of T= 0.4K case. The impurity effect is also reflected partly in the T=1.59K case but overwhelmed by higher temperature in T=4.35K. There is some uncertainty of the interactions ($J_\parallel/J_\perp = (7.7 \pm 1.5)\%$) due to the impurity. As the leg interaction $J_\parallel$ is rather small, the relative uncertainty is quite large. Here we use the values provided in the summary of Ref.[4].
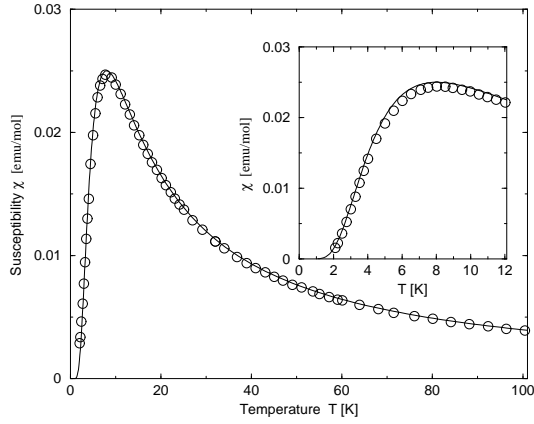

FIG. 4. Magnetic susceptibility versus the temperature for the compounds $(5IAP)_2CuBr_4\cdot2H_2O$, $g = 2.1$, the Curie constant $C = 0.412$ emu K/mol, $J_\perp = 13.0K$, $J_\parallel = 1.0K$. The symbols are the experimental observation, the solid lines are from our calculation. The results for $\gamma = 8/3$ and $1/\gamma = 3/8 - d/4$ do not differ, since the higher orders terms in the gap can be completely ignored due to the weak leg coupling ($J_\parallel/J_\perp \approx 0.077$). Impurity contribution was subtracted in the inset, so the experimental curve is lowered slightly.
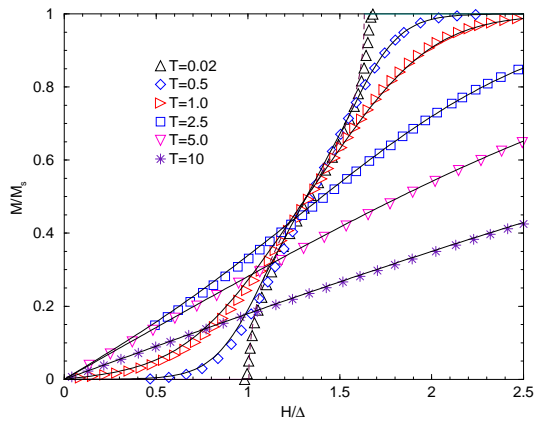

9

FIG. 5. Magnetizations versus the magnetic field at different temperatures in comparison with the transfer-matrix renormalization group (TMRG) numerical result, $J_\perp =5.28$, $J_\parallel =1$ and $\Delta = 4.382$. In this figure the g factor and Bohr magneton μ_B are incorporated in the field H. The data in symbols are TMRG numerical result [11]. The solid lines and the broken line are plotted from our result for $1/\gamma = 3/8 - d/4$ and $\alpha = 1/2$. The GS magnetization is plotted in the broken line in comparison with T=0.02 TMRG data.
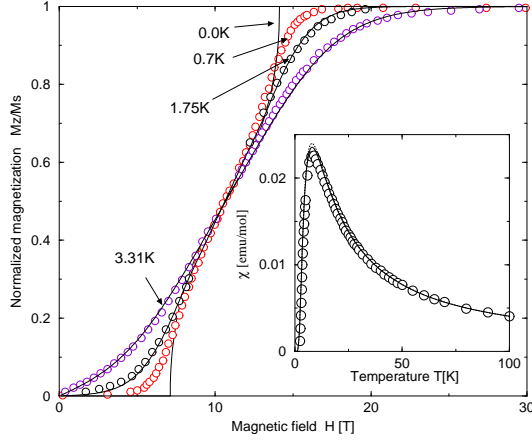

FIG. 6. Magnetizations versus the magnetic field at different temperatures for the compound $(C_5H_{12}N)_2CuBr_4$, $g = 2.13$, $J_\perp = 13.3K$, $J_\parallel = 3.8K$. The symbols denote the experimental data [5]. The solid lines are plotted from our result for $1/\gamma = 3/8 - d/4$ and $\alpha = 1/2$. The difference for the GS magnetization arising from the higher-order terms in the gap can be found in Fig.2B. The inset shows the susceptibility against the temperatures in a low field 0.1T, the Curie constant $C = 0.425$ emu K/mol ($g = 2.13$) [5].The solid line ($1/\gamma = 3/8 - (d + \delta)/4$, $\alpha = 1/2 - \delta$, $\delta = -d/2$) and dotted line ($1/\gamma = 3/8 - d/4$ and $\alpha = 1/2$) have only small difference at the peak.
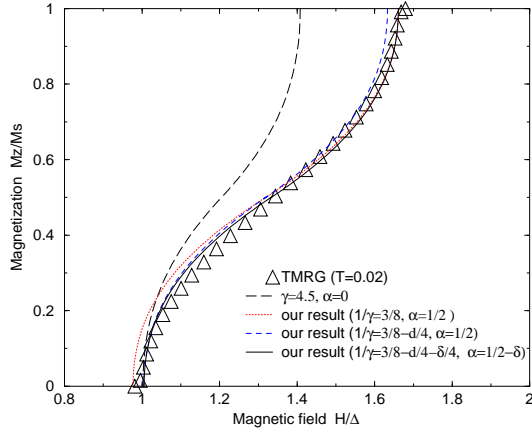

FIG. 7. Groundstate magnetizations in different parameters in comparison with the T=0.02 TMRG result [11] $J_\perp =5.28$, $J_\parallel =1$ and $\Delta = 4.382$. Our reults are plotted according to (13), (21) and (24), respectively, and $\delta = -d/2$ for the solid line. To show their small difference more clearly, we have focused the field on the region between 0.8 and 2.0.
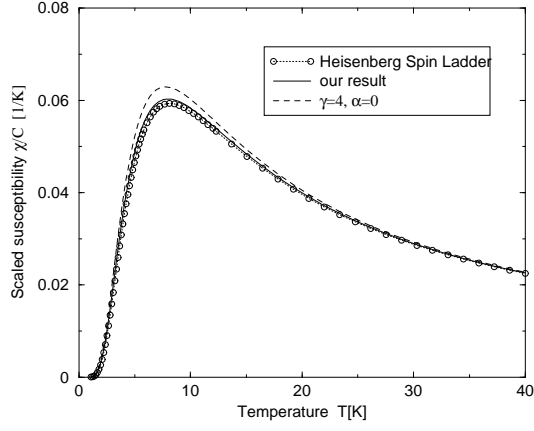
FIG. 8. Scaled magnetic susceptibility against the temperature in comparison with the Heisenberg spin ladder (HSL), $J_\parallel/J_\perp = 0.1$, $J_\perp = 13K$. Since all compounds used in the figures have rung interaction around 13K, we use this value here. For more clarity of the unit, we scale the susceptibility by the Curie constant C. The HSL curve is plotted from the expression (28), which reproduces accurately the quantum Monte Carlo simulations [12] for $J_\parallel/J_\perp \leq 0.1$. Here the high-order terms in the gap make little difference in our result due to the small ratio $J_\parallel/J_\perp$. The agreement for our result with the HSL for stronger coupling $J_\parallel/J_\perp < 0.1$ is even better. The broken line is the result from the choice $\gamma = 4$, $\alpha = 0$, for comparison.